R. Gluckstern (Yale) Computed drift tube shapes

As an introduction a previously used, (approximate) method will be briefly outlined. (Walkinshaw, et.al, AERE reports).

Consider a loaded cavity and define the unit cell as shown.

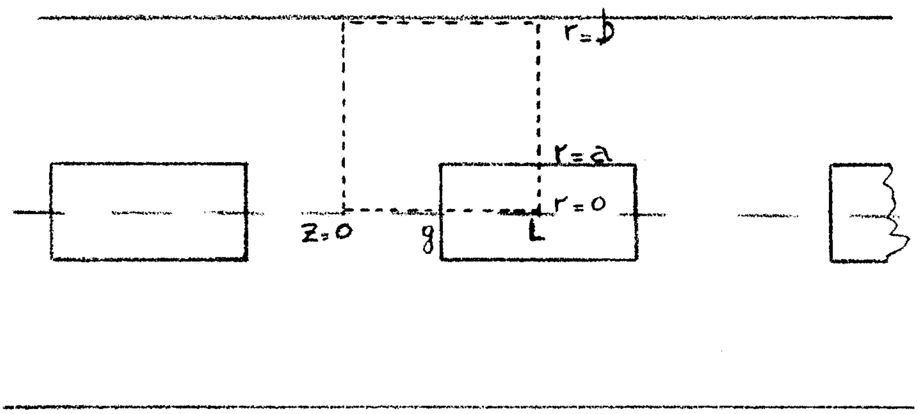

It is necessary now to solve Maxwell's equations such that all E_{tan} components vanish at the walls. This was done by obtaining a Fourier expansion of the field in the two regions inside and outside the drift tube.

i.e.

for the case $r < a$

$$E_z = \sum_{n=o}^{\infty} A_n \cos \frac{n\pi z}{g} \frac{I_o(t_n r)}{I_o(t_n a)} \quad \text{where} \quad t_n^2 = \left(\frac{n\pi}{g}\right)^2 - k^2$$

a further requirement being that

$$E_r = o \quad \text{for } z = o \text{ and } z = g$$

for the region $a < r < b$

$$E_z = \sum_{n=o}^{\infty} B_n \cos \frac{n\pi z}{L} \left[K_o(s_n z) - I_o(s_n r) \frac{K_o(s_n b)}{I_o(s_n b)} \right]$$

where $s_n^2 = \left(\frac{n\pi}{L}\right)^2 - k^2$

$n = o$ leads to imaginary s and t values.

$n > o$ results in a positive value for s_n^2 as a simple substitution with

$k = \frac{2\pi}{\lambda}$ and $2L = \beta\lambda$ will show.

The next step is to impose boundary conditions.

E_z continuous on surface $r = a$ $o < z < g$

E_z equals o on surface $r = a$ $g < z < L$

Further, H_Θ is continuous across the strip $r = a$, $o < z < g$. These conditions require the solution of a determinant of infinite order. For simplicity normally only the term $A_n = A_o$ is used. This leads to a transcendental equation in frequency. Once the frequency is known the field distribution can be deduced. Because only the A_o term is being used the results are approximate only, however, better accuracies can be obtained by using higher order terms.

A refinement of this method has been introduced by N. Christofilos, who used only the part of the drift tube surface perpendicular to the z axis as a starting point, as shown.

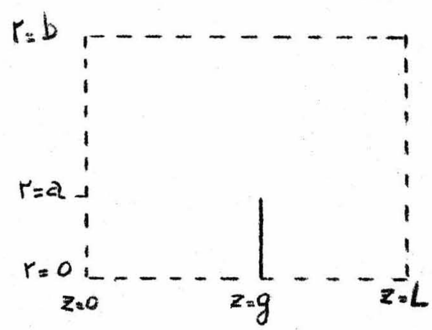

Only 3 or 4 terms in the $E_z = \sum_{n=0}^{\infty} B_n$ ....series were retained.

The coefficients B_n were then adjusted to suit the parameters of the system. This led however to the difficulty that at the matching radius one gets a discontinuity. This is due to the divergence of the series for small r.

The following method is free from these difficulties. Because the drift tube configuration under consideration has the appearance of a set of oscillating dipoles one raises the question what would be the results if one loads a unit cell with a dipole and drives this to establish a field configuration? Perhaps one can then draw surfaces perpendicular to this to obtain the drift tube shapes.

Consider the following case with unit cell as shown :

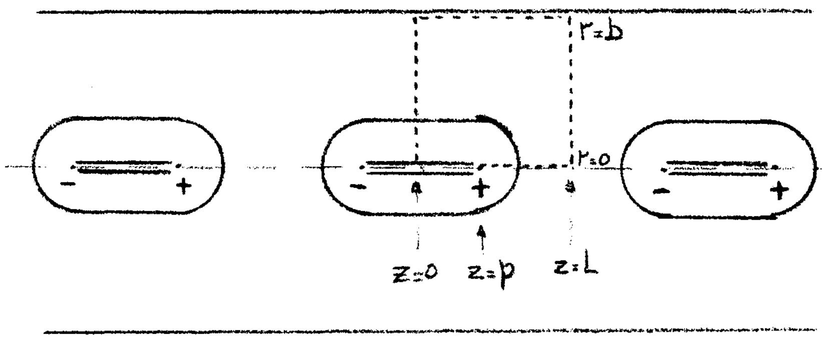

The fields in the unit cell are derived as follows. Only E_z components are being considered, expressions for E_r and H_θ components can be obtained in a completely analogous fashion.

$$\left(\nabla^2 + k^2\right) E_z = \frac{1}{\varepsilon} \nabla_z \rho + i\omega\mu J_z$$

The charge density will be written now as a delta function.

$$\rho = Q\,\delta(z - p)\,\bar{\delta}(r)$$

where $\bar{\delta}(r)$ is given by $\int_0^\infty \bar{\delta}(r)\, 2\pi r \; dr = 1.$

also

$$J_z = i\omega Q\,\Delta(z - p)\,\bar{\delta}(r)$$

defining $\Delta(x) = 1$ for $x > o$

and $\Delta(x) = o$ for $x < o$.

To solve these equations one can follow standard Green's function techniques and write E_z either as a Fourier series in z:

$$E_z(r,z) = \sum_{n=o}^{\infty} \cos\frac{n\pi z}{L}\; A_n(r)$$

or as a series of Bessel functions in r:

$$E_z(r,z) = \sum_{\ell=1}^{\infty} J_o\left(p_\ell \frac{r}{b}\right) B_\ell(z)$$

where p_ℓ are the zero's of J_o.

Substituting $E_z(r,z) = \sum_{n=o}^{\infty}$ .... in the original equation results in

$$\sum_{n=o}^{\infty} \cos\frac{n\pi z}{L}\left[\nabla_\perp^2 - \left(\left(\frac{n\pi}{L}\right)^2 - k^2\right)\right] A_n(r) = \frac{Q}{\varepsilon}\left[\delta'(z-p) - k^2\Delta(z-p)\right]\bar{\delta}(r)$$

Unfolding this series expansion one gets

$$\left(\nabla_\perp^2 - s_n^2\right)A_n(r) = \frac{Q}{\varepsilon}\,\bar{\delta}(r)\,\frac{2}{L}\int \cos\frac{n\pi z}{L}\left(\left(\delta'(z-p) - k^2\Delta(z-p)\right)\right)dz\,*$$

The integral part of this equation will yield simply by partial integration. The next step is to find solutions of the resulting homogeneous equations

$$A_n\left(\nabla_\perp^2 - s_n^2\right)\left[K_o(s_n r) - I_o(s_n r)\frac{K_o(s_n a)}{I_o(s_n a)}\right] = \frac{2Q}{\varepsilon L}\,\bar{\delta}(r)\frac{s_n^2}{n\pi/L}\sin\frac{n\pi p}{L}*$$

Multiplying this by dx dy and integrating, one obtains an expression for A_n and consequently for E_z.

E_z is written below separating the n=o term in the Fourier expansion.

$$E_z = \frac{Q}{\varepsilon\lambda^2}\left\{\frac{\pi^2 p}{L}\left[Y_o(kr) - J(kr)\frac{Y_o(kb)}{J_o(kb)}\right] + \frac{\lambda^2}{\pi^2}\sum_{n=1}^{\infty}\frac{(s_n^2)\sin\frac{n\pi p}{L}\cos\frac{n\pi z}{L}}{n}\right.$$

$$\left.\cdot\left[K_o(s_n r) - I_o(s_n r)\frac{K_o(s_n b)}{I_o(s_n b)}\right]\right\}$$

The convergence of the expansion goes approximately with $e^{-\frac{n\pi r}{L}}$.

This expansion gives fields everywhere in the unit cell but leads to divergent fields along the axis between z=o and z=p. This can be countered by using the second series expansion $E_z = \sum_{\ell=1}^{\infty}$ .... The result is in the form of two types of solutions:

$$\text{for } z > p \qquad E_z = \sum_{\ell=1}^{\infty} J_o\left(p_\ell \frac{r}{b}\right)B_\ell \cosh q_\ell (L-z)$$

$$z < p \qquad E_z = \sum_{\ell=1}^{\infty} J_o\left(p_\ell \frac{r}{b}\right)\left[C_\ell \cosh q_\ell z + D_\ell\right] \text{ with } q_\ell^2 = (p_\ell^2/b^2) - k^2$$

These solutions have to be matched but need not necessarily be continuous across z = p, however $\frac{\partial E_z}{\partial z}$ is continuous.

* Multiply the right hand side of this equation by 1/2 for n = o.

This series development leads to the following expression for E_z for the case $z > p$.

$$E_z = \frac{Q}{\varepsilon\lambda^2}\left\{-\frac{\lambda^2}{\pi b^2}\sum_{\ell=1}^{\infty}\frac{J_0\left(p_\ell \frac{r}{b}\right)}{J_1^2(p_\ell)}\;\frac{p_\ell^2 \sinh q_\ell p}{q_\ell^2\, b^2 \sinh q_\ell L}\cosh q_\ell (L-z)\right\}$$

The convergence of this expression goes approximately with $e^{-\frac{\ell\pi}{b}(z-p)}$

A typical field pattern is sketched below in a unit cell.

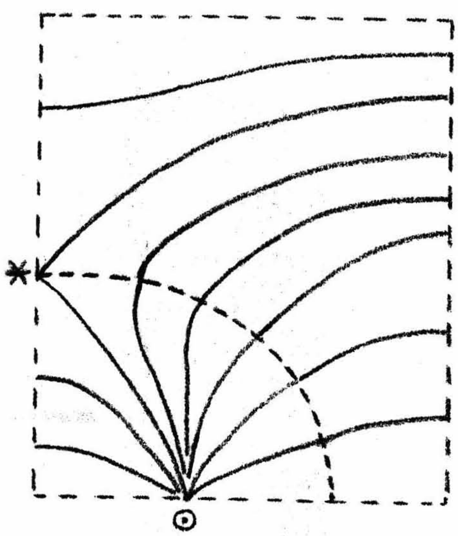

⊙ charge singularity

* nodal point

The dashed line indicates the resulting drift tube surface, of necessity originating at the nodal point of E_z along z=o

Having found the drift tube surfaces one can calculate the fields everywhere and determine losses of the structure.

The described method seems to lend itself to the possibility of superimposing dipoles and then obtaining the fields. Explorations are under way to use linear combinations.

At present it is deemed necessary to use up to 100 terms in the series expansio to obtain sufficiently accurate results.*

Perturbations due to drift tube bore and drift tube stems are considered to be no problem because these are open to approximate calculations.

A typical set of drift tubes for $\beta = 0.6$, $\frac{b}{\lambda} = 0.3$ is shown on the next page.

* The computer time needed to obtain a typical drift tube configuration is about 4 minutes.

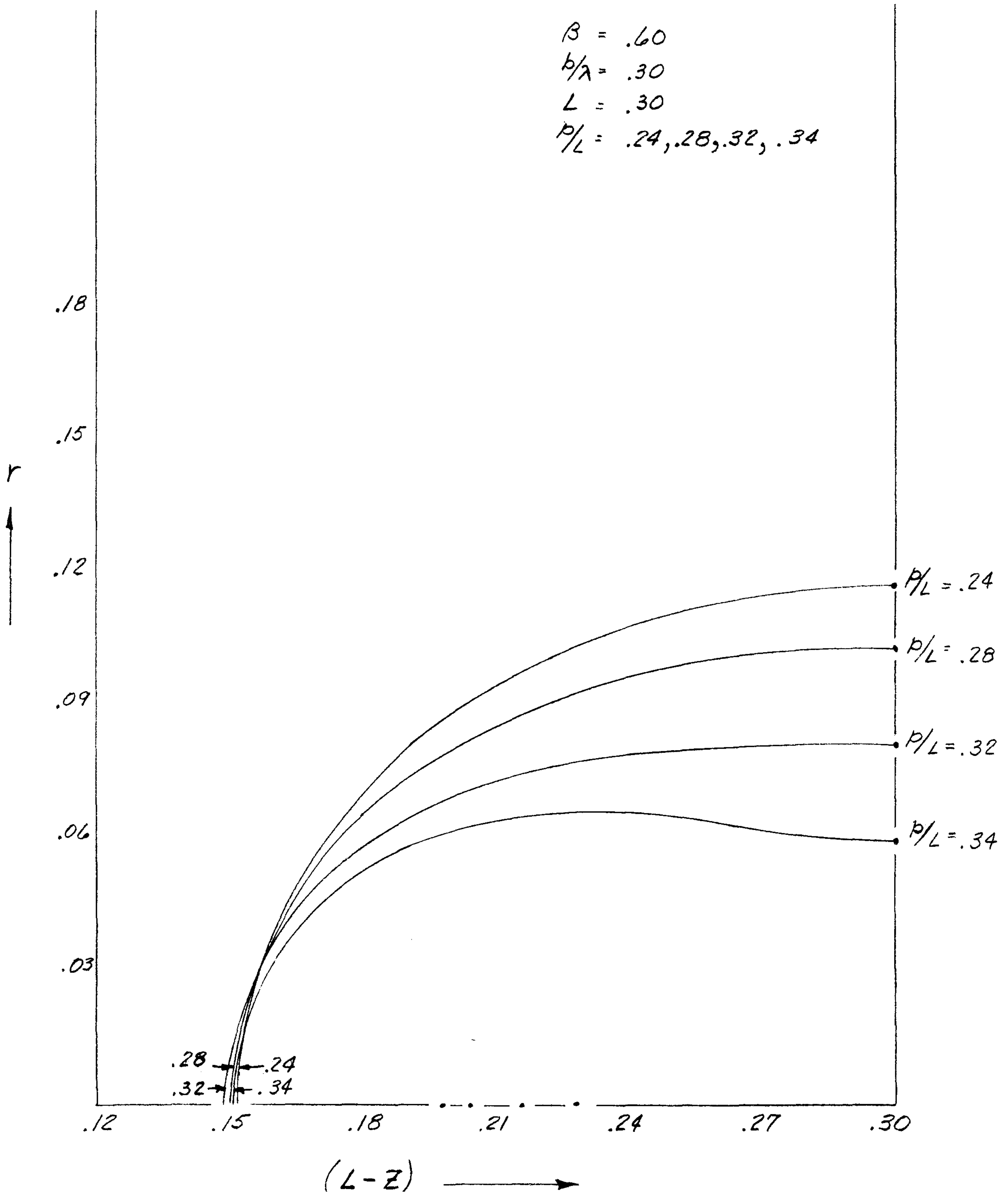
β = .60
b/λ = .30
L = .30
p/L = .24, .28, .32, .34
r
.18
.15
.12
.09
.06
.03
p/L = .24
p/L = .28
p/L = .32
p/L = .34
.28
.24
.32
.34
.12
.15
.18
.21
.24
.27
.30
(L - Z)

The described method lends itself also to an iris loaded, π-mode, standing wave structure.

Consider the following:

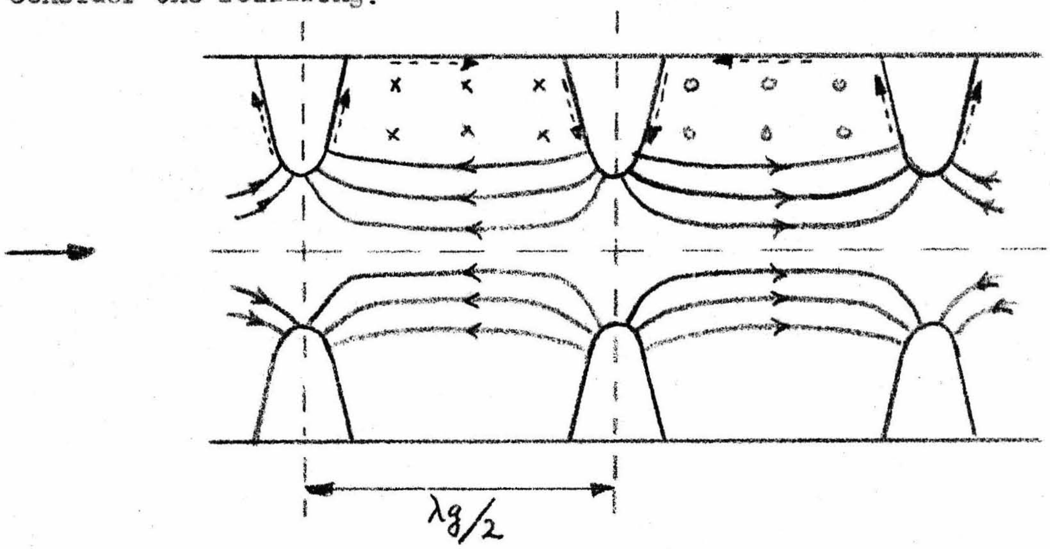

This can be simplified to, with unit cell as shown.

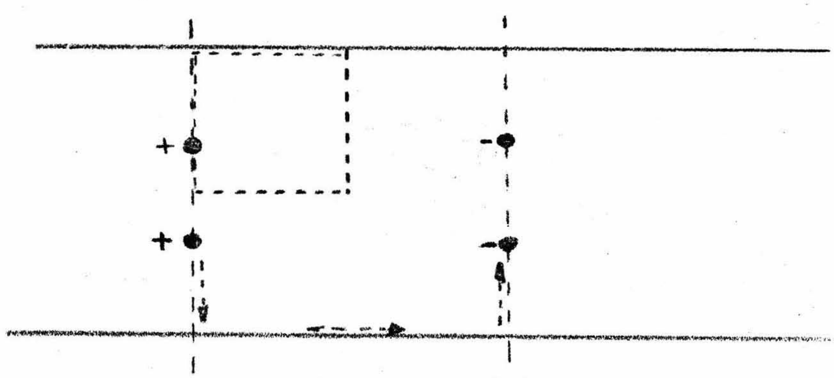

Several cases were treated with the following typical result.

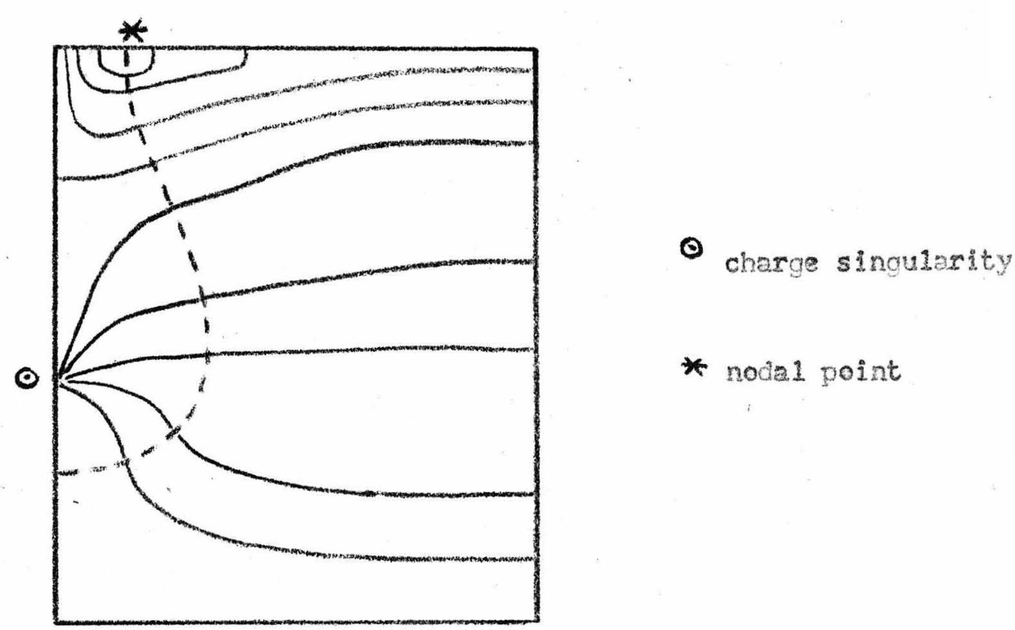

The combination of iris and quadrupole drift tube loaded structure has also been treated by the same method with an appropriate distribution of charges and current. A typical result here is:

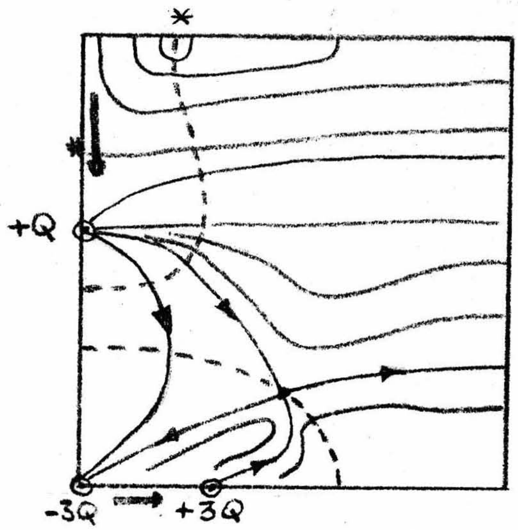

⊙ charge singularity

* nodal point

As a general conclusion it can be said that the described method would work most favorably with a π-mode standing wave structure. At first approach the mathematical problems become rather involved for an iris loaded $\pi/2$-mode standing wave structure or a $\pi/2$-mode taveling wave structure. However, it may be possible to draw approximate conclusions regarding the $\pi/2$ mode cases.